IFSCC 2025 full paper (*IFSCC2025-1178*)

Camellia chrysantha Flower Extract: A Novel Botanical Active for Sensitive Skin Management through Barrier Repair and Anti-Aging Mechanisms

Jianhua Zhang [1,2,*], Shichao Liu [1,2], Wenjiao Guo [1,2], Jing Liu [1]

1 N.O.D topia (GuangZhou) Biotechnology Co., Ltd. Guangdong Guangzhou, 510000, China
2 Simpcare (GuangZhou) Biotechnology Co., Ltd. Guangdong Guangzhou, 510000, China

---

1. Introduction

The skin barrier, a crucial physical defense against external environmental insults, maintains structural integrity that directly influences the body's immune homeostasis and tissue health. Comprising the epidermis, dermis, and subcutaneous tissue layers [1], the barrier system functions in concert to maintain skin physiological function via dynamic homeostasis [2]. However, continuous exposure to exogenous stressors—including physical factors (UV radiation, extreme temperatures), chemical agents (environmental pollutants, hard water), and biological factors (circadian rhythm disruption, psychological stress) can synergistically impair the core components of the skin barrier, resulting in cumulative damage across multiple dimensions, such as oxidative stress, inflammatory responses, and extracellular matrix degradation. This pathological state is characterized by sensitive skin syndrome (burning, redness, itching, stinging) and exogenous aging (wrinkles, loss of elasticity, hyperpigmentation), presenting a significant challenge in contemporary skin health management [3]. However, traditional single-mechanism active ingredients (hyaluronic acid, vitamin C derivatives) often fail to meet clinical requirements due to irritancy or limited efficacy, driving the search for naturally occurring multi-targeted actives as a major research trend.

Camellia chrysantha, a national second-grade protected plant endemic to Guangxi, China, is not only a “plant living fossil” coexisting with dinosaurs but also has been documented in the Compendium of Materia Medica and other texts for its medicinal and food homology. Modern pharmacological research indicates that its flower extracts are rich in polysaccharides, polyphenols, saponins, flavonoids, and various amino acids, which possess diverse health benefits associated with trace elements. They demonstrate significant hypoglycemic, immunomodulatory, and free radical scavenging activities. Despite the growing understanding of its medicinal value and the increasing demand for natural and safe ingredients in skincare, research on *Camellia chrysantha* in the skincare field remains scarce.

In this study,*Camellia chrysantha* flower extract (CFE) was applied for the first time in sensitive skin care, and its efficacy in skin barrier repair and anti-aging was comprehensively evaluated. This study aimed to identify a novel natural product with skin barrier repair and anti-aging efficacy. The therapeutic effects and underlying mechanisms were investigated through in vitro experiments and clinical studies, providing new insights into the development of multifunctional natural active ingredients for sensitive skin.

2. Materials and Methods

2.1 DPPH radical scavenging activity assay

Percent radical scavenging activity was assessed using the DPPH protocol [4]. Briefly, a 200 μg/mL DPPH working solution was freshly prepared in anhydrous methanol (HPLC grade) and stored at 4°C in amber vials to prevent photodegradation. CFE stock solutions (10 mg/mL in methanol) were serially diluted to obtain concentration gradients spanning 0.1-100 μg/mL. For experimental trials, 100 μL of each diluted CFE sample was combined with 100 μL of DPPH solution in 96-well microplates, with methanol serving as blank control. After 90 min incubation under a dark conditions at 25±1°C, absorbance was measured at 517 nm using a microplate reader (Molecular Devices). All assays were conducted in triplicate with three independent biological replicates.

Radical scavenging activity (%) was calculated as:

$$\text{DPPH scavenging activity}(\%)=1-\frac{\text{Asample}-\text{Acontrol}}{\text{Acontrol}}\times 100\%$$

2.2 Hyaluronidase inhibitory activity

In this study, the inhibitory activity assay of bovine testicular hyaluronidase (5 mg/mL, dissolved in 0.2 M sodium acetate buffer, pH 5.4) on hyaluronic acid (5 mg/mL) was conducted as follows: To 100 μL of samples or positive controls, 50 μL of hyaluronic acid, 300 μL of buffer, and 200 μL of hyaluronidase were added, respectively. For the blank control group, 50 μL of hyaluronic acid and 100 μL of buffer were added. The enzyme reaction group consisted of 50 μL of hyaluronic acid, 250 μL of buffer, and 200 μL of enzyme solution. For the reaction control group, 100 μL of the corresponding samples and 250 μL of sodium acetate buffer solution were added. Following a 2.5 hour incubation at 37°C, 500 μL of 2.5% cetyltrimethylammonium bromide (CTAB) was added to terminate the reaction and initiate color development. Subsequently, 200 μL of the reaction mixture was transferred to a 96 well plate, and the absorbance was measured at 400 nm using a microplate reader.

$$\text{Enzyme activity inhibition}(\%)=1-\frac{\text{Asample}-\text{Acontrol}}{\text{Acontrol}}\times 100\%$$

2.3 Cell culture

HaCaT cells sourced from BNCC (BeNa Culture Collection). They were cultured in a humidified 5% CO_2, and 95% oxygen atmosphere at 37 °C in Dulbecco's modified Eagle's medium (DMEM, Gibco) supplemented with 10% fetal bovine serum, 2 mM glutamine, 100 U/mL penicillin, and 100 μg/mL streptomycin.

2.4 UVB irradiation model

After determining the safe concentration of the samples via the MTT method, a flask of exponentially growing cells in good condition was selected. 0.25% trypsin digestion solution was added to detach the adherent cells. Subsequently, the cells were counted and adjusted to a concentration of 1–4×10^5 cells/mL to prepare the cell suspension. The cell suspension was inoculated into 12-well plates and incubated in a CO_2 incubator for 24 h. Thereafter, the complete medium in the wells was aspirated, replaced with PBS, and then the cells were exposed to UVB light for 15 min. For the blank control group, the complete medium was retained without irradiation. Following the 15 min UVB irradiation, the PBS solution was aspirated, and different concentrations of the test material were added to the experimental group. The control group received complete medium, and both groups were incubated for 48 h. Finally, the experimental group underwent an additional 15 min of UVB irradiation.

2.5 ELISA assay

Cells were collected and centrifuged to pellet the cells. The supernatant was discarded, and RIPA lysate was added to the cell pellet. The mixture was vortexed three times (30 seconds each, with a 3 minute interval between each vortexing) and then centrifuged at 12,000 rpm for 10 minutes. The supernatant was collected and subjected to detection using an ELISA kit. Subsequently, the total protein concentration of the supernatant was determined with a BCA protein quantification kit. The expression levels of filaggrin (FLG), loricrin (LOR) and MMP-1 were analyzed using an ELISA kit. The supernatants of each cell culture group were collected and centrifuged at an appropriate speed for 5 minutes to remove cell debris. All experiments were performed in triplicate according to the manufacturer's instructions.

2.6 Clinical trial

For each experiment, eligible subjects were screened who were between 30 and 50 years of age, understood the content of the test, voluntarily agreed, signed an informed consent form, and followed the test protocol. Subjects were placed in a controlled environment with a temperature range of 20°C-22°C and humidity levels between 40% and 60% RH. Use of 1% CFE to formulate emulsions for subsequent human experiments.

2.6.1 Patch test

A total of 33 healthy subjects were enrolled in this study. The subjects were acclimatized to a controlled environment with a temperature for 30 minutes. Qualified patch-testing devices with an area not exceeding 50 mm² and a depth of approximately 1 mm were selected. The test material (0.020 - 0.025 g) was placed in the small chamber of the patch tester. The patch was applied to the flexor aspect of both forearms and occluded. The skin reactions were observed 30 minutes after patch removal at 24 hour and 48 hour time points, respectively, once the indentation had disappeared, and the observation results were recorded.

2.6.2 Human Soothing Efficacy Assessment

Subjects were allowed to rest for 15 minutes in a constant temperature and humidity environment. During the pre-screening phase, 10% ethanol soaked swabs were laterally rubbed five times along the nasolabial folds at 1 cm intervals within 2 minutes to exclude subjects reporting immediate discomfort. Subsequently, 50 μL droplets of a 0.01% (w/v) capsaicin solution were placed on a filter paper sheet with a diameter of 0.8 cm and applied 1 cm lateral to the nasolabial folds. The filter paper was removed after 3 minutes.The intensity of the burning sensation was evaluated using a 5 point scale. Subjects with a score of ≥3 on the stimulated side, with the sensation lasting >30 seconds, were classified as capsaicin test positive (CATP), while the remaining subjects were classified as capsaicin test negative (CATN). TEWL values, erythema values, and capsaicin stimulation self-assessment score were measured on day 0, day 14, and day 28 in both the test sample and placebo groups for eligible enrolled subjects.

2.6.3 Human firming and anti-wrinkle efficacy assessment

A total of 33 physically healthy male and female subjects were recruited for the study. Subjects were randomly assigned to either the experimental group or the placebo group to ensure that at least 30 subjects completed the entire follow-up period (D14, D28, D56). During each visit, subjects washed their faces with the specified cleansing solution in a controlled environment and remained sedentary for 30 minutes. Subsequently, instruments were used to

measure the R2, R7, and Q1 values of skin elasticity, as well as the wrinkle area and length (including eye corner, under-eye lines, and nasolabial folds) in both the placebo and CFE groups after 14, 28, and 56 days of product application.

2.7 Statistical analysis

In this study, results are presented as mean ± SEM. Mean values were calculated based on data from at least three independent replicated experiments. Data were analyzed using GraphPad Prism 7 and SPSS 26.0. The results were subjected to an analysis of variance (ANOVA) using the Tukey's test to analyze difference. $P < 0.05$ indicates a statistically significant difference. In the analysis of results, * denotes comparison with control or baseline, $P < 0.05$; ** denotes comparison with control or baseline, $P < 0.01$.

3. Results

3.1 In vitro antioxidant evaluation results

In this study, the antioxidant potential of CFE was evaluated using the DPPH method. All five tested concentrations of CFE demonstrated strong antioxidant capacity (Figure 1). A significant dose-dependent relationship was observed, and the data were statistically significant ($p < 0.05$). With VC as the positive control, the IC_{50} values of CFE and VC were 1.96 and 1.02, respectively.

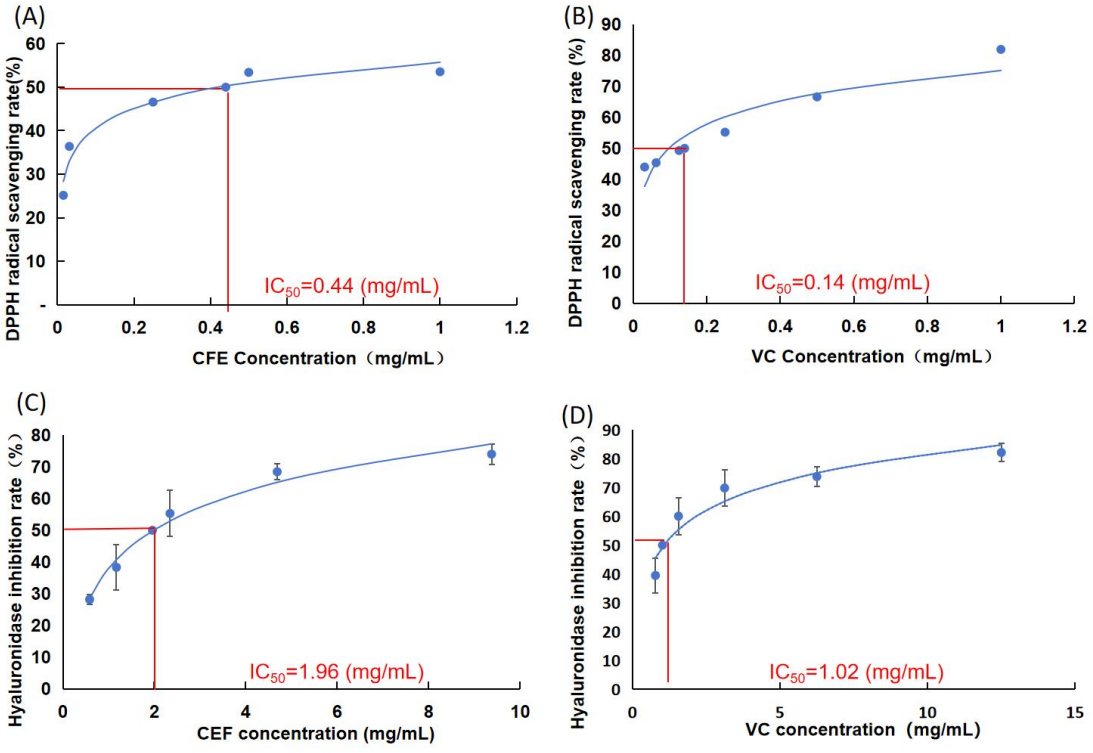

Figure 1. The ability of CFE (A) and VC (B) scavenging free radical assays was examined using the DPPH method. Hyaluronidase inhibitory activity was examined for CFE (C) and VC (D).

3.2 In vitro soothing efficacy evaluation results

Hyaluronidase inhibitory activity was evaluated to assess the soothing effect of CFE. The results showed a significant dose-dependent relationship, and with VC as the positive control, the IC50 values of CFE and VC were 0.44 and 0.14, respectively. The bioactivity assessment indicated that CFE exhibited good soothing effects.

3.3 Anti-photoaging effect of CFE on UVB exposed HaCaT cells

As depicted in Figure (2), the cell viability of HaCaT cells treated with CFE was assessed by the CCK-8 assay. Based on the results, 20 and 50 ppm concentrations, which showed no cytotoxicity at 24 hours, were chosen as the test concentrations for subsequent experiments. The experimental results indicated that, in the UVB-irradiated cellular photoaging model, the 20 ppm CFE significantly enhanced the FLG expression in HaCaT cells compared to the UVB only group, demonstrating a FLG expression effect. Conversely, both 20 ppm and 50 ppm CFE significantly elevated the LOR content in HaCaT cells, Indicating improved LOR expression. Compared with the UVB group, the 50 ppm CFE could reduce the MMP-1 content in cells to some extent, yet the reduction was not statistically significant.

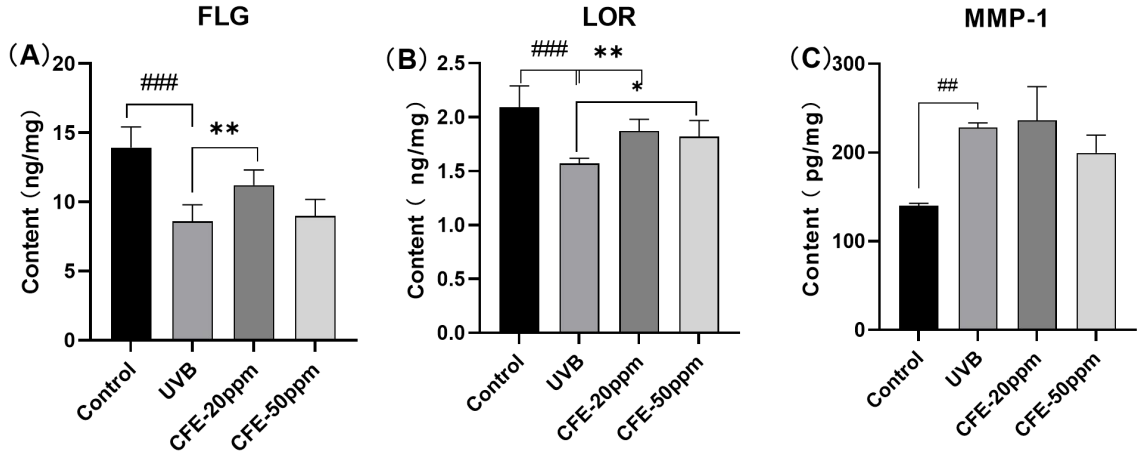

Figure 2. After exposure to UVB (20 mJ/cm^2), cells were treated with CFE for 24 h and the levels of FLG (A), LOR (B), and MMP-1 (C) were determined by using an Elisa kit. All results are expressed as mean ± standard deviation. ### p < 0.01 , ## *P* < 0.05 Compared with the positive control group. **P* < 0.05,** *P* < 0.01,** *P* < 0.001. Compared with the negative control group.

3.4 Human efficacy evaluation

As shown in Figure 3, after 14 and 28 days of treatment, the CFE group demonstrated marked reductions in TEWL by 29.41% and 39.29%, respectively, compared to day 0 (*P* < 0.01). In contrast, the placebo group showed only modest TEWL reductions of 6.68% at day 14 and 10.00% at day 28. Similarly, erythema values showed a 5.19% reduction at day 14 (*P* < 0.01) and 6.66% at day 28 (*P* < 0.05) in the CFE group, whereas the placebo group demonstrated a 0.43% increase (day 14) and 2.39% reduction (day 28), neither of which reached statistical significance (both *P* > 0.05)..As shown in Figure 3C, capsaicin stimulation score demonstrated significant improvements in the CFE group. After 14 days of treatment compared to day 0, the test area showed a 27.31% reduction in stimulation score (*P* < 0.05),

whereas the placebo group exhibited only a 15.22% decrease. By day 28, the CFE group achieved a highly significant 41.02% reduction ($P < 0.01$), while the placebo group showed a 27.58% change in capsaicin stimulation scores ($P > 0.05$).

The CFE group demonstrated time dependent improvements in skin elasticity parameters (Figure 4). R2 values (Figure 4A) showed progressive enhancement from 7.55% at day 14 to 19.40% at day 56 ($P < 0.001$ vs day 0). R7 values (Figure 4B) reached statistical significance at day 28 (6.80% improvement, $P < 0.01$) with further elevation to 16.70% by day 56 ($P < 0.001$). Q1 values (Figure 4C) exhibited sustained increases from 6.21% (day 14, $P < 0.01$) to 17.77% (day 56, $P < 0.001$). In contrast, the placebo group displayed progressive deterioration of skin elasticity, particularly evident at day 56 with significant reductions in R2 (-3.53%), R7 (-5.42%), and Q1 (-4.22%) values (all $P < 0.05$).

As shown in Figure 5 by evaluating the clinical data at 14, 28, and 56 days, it was evident that the CFE group showed a significant improvement ($P <0.01$) in Wrinkle Area and Wrinkle Length in each of the observed areas (corners of the eyes, under-eye , and nasolabial folds). This was demonstrated by a 9.88% and 11.16% reduction in wrinkle area and length at the corners of the eyes, respectively, at 56 days, along with a reduction in the length of the decree lines of up to 12.94% (all $P <0.05$). Compared to the placebo group: wrinkle area and length were significantly reduced in the CFE group at 14 days, and the difference between the two groups reached a maximum at 56 days ($P <0.001$). Notably, while the placebo group showed a 6.04% improvement in the length of under-eye wrinkles at 56 days, the improvement in the CFE group (9.20%) remained significantly better (all $P <0.001$). Statistical analysis confirmed that the CFE group was significantly better than the placebo group ($P <0.05$) in all measures tested at both 28 and 56 days, particularly in terms of improvement in nasolabial folds, with the CFE group significantly outperforming the placebo group in terms of wrinkle area and length reductions at 56 days (7.53%; 12.94%) over the placebo group's 0.61% elevation and 1.99% elevation ($P <0.001$).

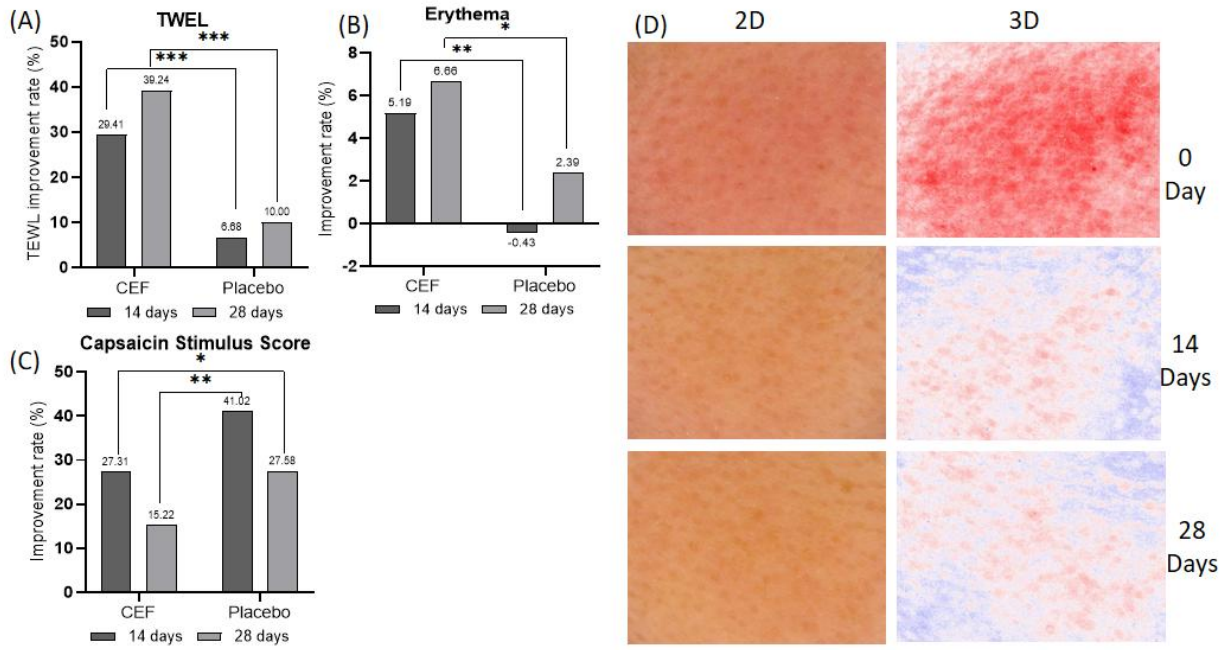

Figure 3. Effects of CFE and placebo on skin parameters. (A) The improvement rate of TEWL

at days 14 and 28; (B) The improvement rate of erythema at days 14 and 28; (C) The improvement rate of stinging score at days 14 and 28; (D) The representative images of the skin at days 0 and 28. N = 30. Student t-test, * $P < 0.05$, ** $P < 0.01$, *** $P < 0.001$ vs. placebo. * Skin reaction scoring criteria: No reaction.

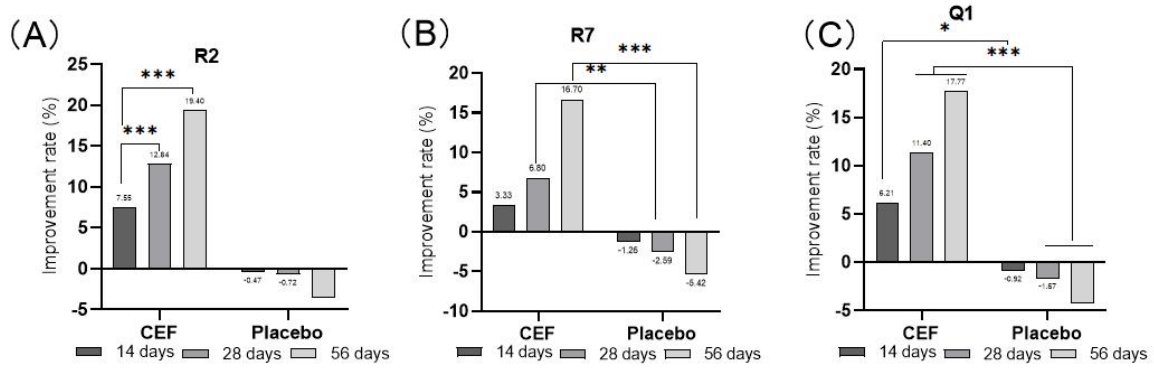

Figure 4. Effects of CFE and placebo on skin elasticity parameters.(A) Improvement rate of R2 value. (B) Improvement rate of R7 value. (C) Improvement rate of Q1 value. N = 30. Compared to the placebo group, * $P < 0.05$, ** $P < 0.01$, *** $P < 0.001$ vs. placebo.

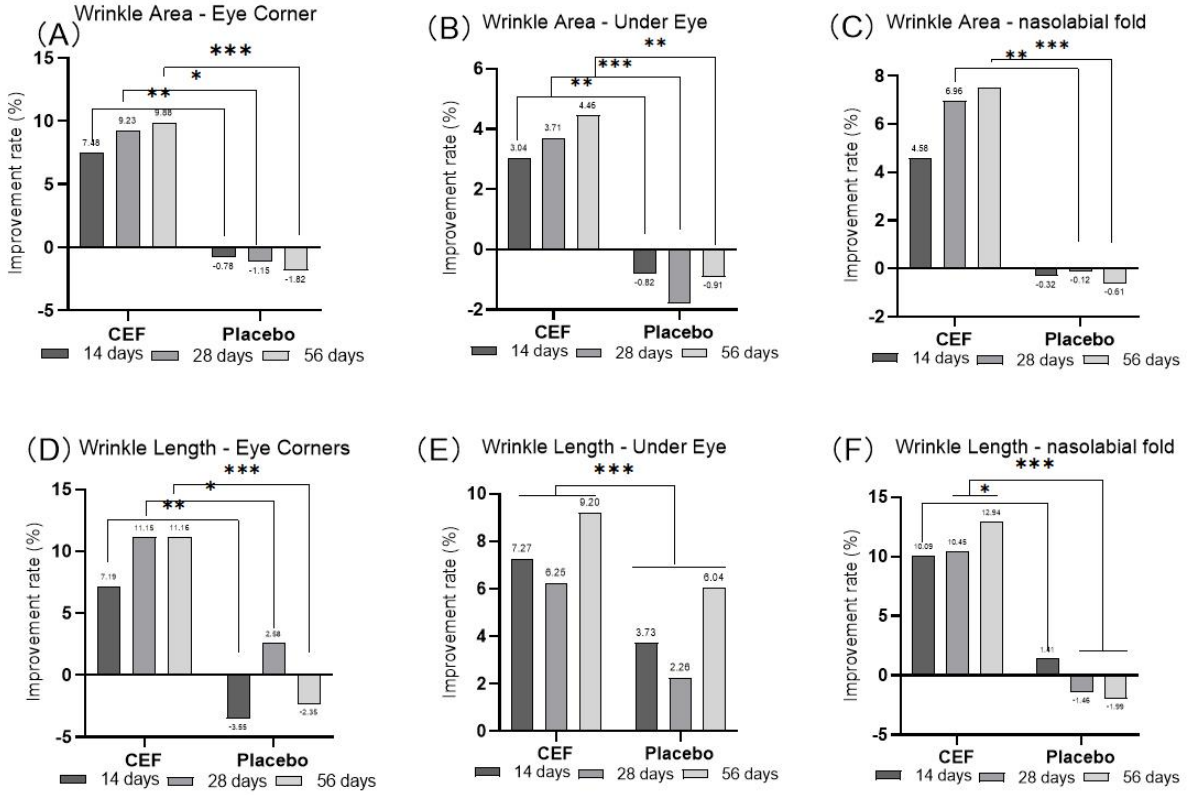

Figure 5. Effects of CFE and placebo on skin wrinkle parameters.(A) Improvement rate of wrinkle area for eye corner. (B) Improvement rate of wrinkle area for under eye. (C) Improvement rate of wrinkle area for nasolabial folds. (D) Improvement rate of wrinkle length

for eye corners. (E) Improvement rate of wrinkle length for under eye area. (F) Improvement rate of wrinkle length for nasolabial folds. Compared to the placebo group, *p<0.05, **p<0.01, ***p<0.001.

4. Discussion

Numerous studies have shown that naturally sourced plant extracts contain a wide range of active ingredients, such as polysaccharides [5], flavonoids [6], polyphenols [7,8], and amino acids. These components are well - known for their moisturizing, whitening, soothing, and anti -aging properties. The application of plant - derived active ingredients in dermatology, an emerging research direction, also demonstrates great potential in treating system - related diseases. For example, *potato exosomes* (ExoPs) have been shown to penetrate keratinocytes (HaCaT) and inhibit the expression of collagen - degrading enzymes (MMP-1, 2, 9) and inflammatory cytokines (IL - 6, TNF - α), effectively reversing UVB radiation damage [9]. This study employed an integrated evaluation strategy, including in vitro antioxidant activity assessment, soothing efficacy measurement, anti-photoaging analysis, and clinical efficacy testing, to investigate the barrier - repair and anti-aging mechanisms of CFE. Reactive Oxygen Species (ROS), mainly including hydroxyl radicals, superoxide anions, and hydrogen peroxide, are generated in the skin upon UV irradiation. ROS induce oxidative stress damage, which is a major clinical manifestation of photoaging. Our results indicate that CFE exhibits antioxidant properties, effectively scavenging various ROS and preventing oxidative stress - induced damage, thereby counteracting skin photoaging [10].

The present study also demonstrated that CFE inhibits the activities of hyaluronidase and collagenase. These enzymes are responsible for degrading hyaluronic acid and collagen, respectively. External factors such as UV irradiation and aging reduce the levels of hyaluronic acid and collagen, leading to the deterioration of skin structure and function. Therefore, the inhibitory effect of CFE on hyaluronidase and collagenase suggests its role in promoting the biosynthesis of collagen and hyaluronic acid, thus maintaining skin integrity [11].UVA and UVB are the primary exogenous factors contributing to photoaging, directly affecting cell differentiation, growth, and senescence, and ultimately causing tissue degradation [12]. Our findings revealed that CFE significantly upregulated the expression of FLG and LOR in UVB - irradiated HaCaT cells. FLG serves as a precursor protein for the natural moisturizing factor in the stratum corneum, while LOR participates in the cross - linking of the keratin envelope. These two proteins work synergistically to enhance the skin's physical barrier. Meanwhile, in vitro experiments showed that CFE inhibited hyaluronidase activity, reducing hyaluronic acid degradation. Collectively, these results suggest that CFE may ameliorate skin aging by alleviating oxidative stress caused by external stimuli. The in vitro DPPH free - radical scavenging assay further confirmed the potent antioxidant capacity of CFE. Previous research has identified anti-wrinkle properties in various natural extracts. For example, the leaf ethanol extract of *Aceriphyllum rossii*, a Korean endemic perennial herb, exerts anti - wrinkle effects by upregulating type I procollagen synthesis and inhibiting the activities of collagenase, elastase, and MMP-1 in human dermal fibroblasts [13]. The aqueous extract of tuna heart exhibits anti - aging and anti - wrinkle effects on human fibroblasts by reducing elastase activity and increasing the expression of tissue inhibitors of MMP - 1 and promoting collagen synthesis [14]. Libidibia ferrea (jucá) bark and pod extracts, which possess potent antioxidant and enzymatic inhibitory activities, demonstrate anti - wrinkle and anti - whitening effects through their inhibitory effects on hyaluronidase, pro-MMP - 2, and tyrosinase [15]. Although the exact mechanism remains to be elucidated, the anti - wrinkle properties of A. rugosa proposed in this study are presumably associated with its antioxidant activity. The

barrier protection of sensitive skin is a key focus in the development of functional cosmetics. Both in vitro and clinical experiments demonstrated that CFE possesses excellent barrier - repair capabilities. We hypothesize that this effect is attributed to the rich content of polysaccharides [16-19], polyphenols, and other bioactive substances in CFE, all of which contribute to barrier repair.

CFE has distinct advantages over other plant extracts. Unlike some plant extracts with single - function properties, such as antioxidant or anti - inflammatory effects, CFE combines antioxidant, anti - inflammatory, soothing, and anti - wrinkle properties. The synergistic action of its various bioactive components enables it to exert multiple beneficial effects on the skin, making it a highly versatile ingredient in skincare products. However, this study has several limitations. Based on the current experimental data, CFE shows great promise as an effective ingredient for antioxidant, anti - aging, soothing, and anti - wrinkle skincare products. Future research should expand the scope of investigation, including conducting larger - scale clinical trials, exploring the underlying molecular mechanisms in depth, and developing optimized formulations to maximize the efficacy of Camellia sinensis extract. These efforts will deepen our understanding of CFE's properties and facilitate its broader application in the cosmetic and skincare industry.

5. Conclusion

Although the current work has demonstrated, for the first time, the efficacy of CFE as a skin care ingredient in skin barrier repair and anti-aging through in vitro efficacy and clinical trials, the specific mechanism of action needs to be explored in greater depth. Our current study concludes that CFE is able to protect cells from oxidative stress caused by ROS generated by UVB radiation through free radical scavenging ability while improving TEWL, erythema and stinging scores in sensitive skin. Therefore, these results provide a possibility for the use of CFE as a skin care ingredient with skin barrier repair and anti-aging benefits.

References

1. Slominski A., Tobin D.J., Shibahara S., Wortsman J. Melanin pigmentation in mammalian skin and its hormonal regulation. Physiol. Rev. 2004;84:1155–1228.
2. Fluhr JW, Moore DJ, Lane ME, Lachmann N, Rawlings AV. Epidermal barrier function in dry, flaky and sensitive skin: A narrative review. J Eur Acad Dermatol Venereol. 2024;38(5):812-820.
3. Meghe SR, Khan A, Jangid SD, Sarda B, Vangala N, Saoji V. Shedding Light on Acne Scars: A Comprehensive Review of CO2 vs. Erbium-Doped Yttrium Aluminium Garnet (Er:YAG) Laser Therapy. Cureus. 2024;16(4):e57572.
4. Wong SP, Leong LP, Koh JHW.. Antioxidant activities of aqueous extracts of selected plants. Food Chem. 2006;99(4):775–783.
5. Chen S, Xi M, Gao F, et al. Evaluation of mulberry leaves' hypoglycemic properties and hypoglycemic mechanisms. Front Pharmacol. 2023;14:1045309. Published 2023 Apr 6.
6. Lee CF, Fan CW, Chiang NN, et al. Protective effect of Corchorus capsularis L. leaves on ethanol-induced acute gastric mucosal lesion in rats. J Vet Med Sci. 2019;81(11):1636-1642.
7. Yang C, Zhu X, Liu W, et al. Dietary Dried Jujube Fruit Powder (DJFP) Supplementation Improves Growth Performance, Antioxidant Stability, and Meat Composition in

Broilers. Foods. 2023;12(7):1463. Published 2023 Mar 29.
8. Zielińska A, Nowak I. Abundance of active ingredients in sea-buckthorn oil. Lipids Health Dis. 2017;16(1):95.
9. Takatsuka, M., Goto, S., Kobayashi, K., Otsuka, Y., and Shimada, Y. (2022). Evaluation of pure antioxidative capacity of antioxidants: ESR spectroscopy of stable radicals by DPPH and ABTS assays with singular value decomposition. Food Biosci. 48,
10. Yoshihara, M., Kawakami, S., Matsui, Y., and Kawama, T. (2024). Piceatannol enhances hyaluronic acid synthesis through SIRT1-Mediated HAS2 upregulation in human dermal fibroblasts. Biochem. Biophys. Rep. 39,
11. Videira I.F.d.S., Moura D.F.L., Magina S. Mechanisms regulating melanogenesis. Anais Brasil. Dermatol. 2013;88:76–83.
12. Guo, K., Liu, R., Jing, R., Wang, L., Li, X., Zhang, K., et al. Cryptotanshinone protects skin cells from ultraviolet radiation-induced photoaging via its antioxidant effect and by reducing mitochondrial dysfunction and inhibiting apoptosis. Front. Pharmacol
13. Ha B. G., Park M. A., Lee C. M., Kim Y. C. Antioxidant activity and anti-wrinkle effects of Aceriphyllum rossii leaf ethanol extract. Toxicological Research. 2015;31(4):363–369.
14. Kim Y.-M., Jung H.-J., Choi J.-S., Nam T.-J. Anti-wrinkle effects of a tuna heart H2O fraction on Hs27 human fibroblasts. International Journal of Molecular Medicine. 2016;37(1):92–98.
15. do Nascimento Pedrosa T., Barros A. O., Nogueira J. R., et al. Anti-wrinkle and anti-whitening effects of jucá (Libidibia ferrea Mart.) extracts. Archives of Dermatological Research. 2016;308(9):643–654.
16. Zhao XY, Zhang F, Pan W, Yang YF, Jiang XY. Clinical potentials of ginseng polysaccharide for treating gestational diabetes mellitus. World J Clin Cases. 2021;9(19):4959–4979.
17. Wu M, Li W, Zhang Y, et al. Structure characteristics, hypoglycemic and immunomodulatory activities of pectic polysaccharides from Rosa setate x Rosa rugosa waste. Carbohydr Polym. 2021;253:117190
18. Nai J, Zhang C, Shao H, et al. Extraction, structure, pharmacological activities and drug carrier applications of Angelica sinensis polysaccharide. Int J Biol Macromol. 2021;183:2337–2353.
19. Liu Y, Li H, Zheng Z, et al. Rosa rugosa polysaccharide induces autophagy‐mediated apoptosis in human cervical cancer cells via the PI3K/AKT/mTOR pathway. Int J Biol Macromol. 2022;212:257–274.